In situ investigation of optical absorption changes in $LiNbO_3$ during reducing/oxidizing high-temperature treatments

2007 J. Phys.: Condens. Matter 19 086211

(http://iopscience.iop.org/0953-8984/19/8/086211)

IOP PUBLISHING JOURNAL OF PHYSICS: CONDENSED MATTER

J. Phys.: Condens. Matter **19** (2007) 086211 (12pp) doi:10.1088/0953-8984/19/8/086211

In situ investigation of optical absorption changes in $LiNbO_3$ during reducing/oxidizing high-temperature treatments

D Sugak[1], Ya Zhydachevskii[2], Yu Sugak[2], O Buryy[2], S Ubizskii[2], I Solskii[1], M Schrader[3] and K-D Becker[3]

[1] Institute of Materials, SRC 'Carat', 202 Stryjska, Lviv, 79031, Ukraine
[2] Lviv Polytechnic National University, 12 Bandera, Lviv, 79013, Ukraine
[3] Institute of Physical and Theoretical Chemistry, Technical University Braunschweig, Braunschweig, D-38106, Germany

E-mail: crystal@polynet.lviv.ua (O Buryy)

Received 17 October 2006, in final form 10 January 2007
Published 9 February 2007
Online at stacks.iop.org/JPhysCM/19/086211

Abstract

This paper presents experimental results of an *in situ* investigation of optical absorption of congruent lithium niobate during reducing (95% Ar + 5% H_2) and oxidizing (O_2) high-temperature treatments in the temperature range from 20 to 800 °C. The absorption spectra measured at *in situ* conditions at high temperatures in reducing/oxidizing atmospheres as well as the kinetics recorded at fixed wavelength during rapid replacement of gas atmospheres have been analysed. The origin of the changes in optical absorption caused by the redox treatments is discussed in terms of hydrogen and oxygen ion diffusion and the point defect structure of the material.

1. Introduction

The sensitivity of lithium niobate (LN) crystals to the influence of external electromagnetic fields is determined by the presence of point defects, including impurity ions, in the crystal structure. Changes of the charge state of point defects and impurity ions under the influence of light serve as a basis for holographic application of LN crystals and of crystals doped with Fe, Mn, Cu and other ions and their combinations [1, 2]. On the other hand, the use of LN crystals in light beam control devices requires an as small as possible sensitivity to radiation. The resistance to radiation damage can be increased in particular by doping with MgO [3]. Hence, an investigation of the defect subsystem and of the influence of electromagnetic fields on the charge and energy transfer processes with participation of point defects and impurity ions is a fundamental task that determines the utilization of LN crystals in optoelectronics. That is why a study into the changes in the defect subsystem in LN under the influence of external factors represents an actual problem of this functional material.

One of the ways to influence the defect subsystem of a crystal is by exposure to different atmospheres (oxidizing, reducing or neutral ones) at high temperatures. Depending on the annealing conditions, the charge state of the point defects and impurity ions can be changed, and new defects can be formed. Such annealing processes are frequently used for the modification of crystal properties. For example, the oxidation/reduction state of LN crystals determines their holographic recording efficiency; variations in this state by appropriate annealing procedures are used for optimizing the crystal for holographic applications [4, 5]. In addition, heating of LN above 100 °C during the holographic recording process allows one to achieve prolonged optical data storage—so-called thermal fixing. The nature of thermal fixing is related to the temperature-induced compensation of the space-separated charges. Diffusion of H^+ ions present in LN crystals is considered as a possible mechanism for inducing such changes [5, 6].

Various atmospheres, such as pure hydrogen [7], argon [4, 8, 9], gas mixtures as for example 90% N_2 + 10% H_2 [10] as well as vacuum [8, 11–14], are usually used for a reducing annealing of LN crystals. The results of all these works regarding the influence of high-temperature reduction on optical properties of LN crystals in general are quite similar: a broad, complex absorption band is observed near 2.5 eV (∼20 000 cm^{-1}). The intensity of this absorption band is found to depend on the temperature and duration of the annealing process [9, 10]. The subsequent annealing of the 'reduced' crystals in oxidizing atmospheres returns them to the colourless state.

When the colouration processes that take place in LN crystals under the influence of external factors were studied, several models of the absorbing centres were considered. One of the first possible explanations of the colouration that arises in the reduced crystals is formation of F^+ and F centres based on oxygen vacancies [8, 12]. However, subsequent experimental and theoretical studies explain the absorption of the reduced crystals by the way of formation of small polarons (an electron trapped at Nb_{Nb} ion) and bipolarons (two electrons captured by Nb_{Li}–Nb_{Nb} traps) [7, 11, 13, 15, 16]. It is known that Nb_{Li} anti-site ions are typical structural defects of congruently grown LN crystals [17]. Theoretical calculations of the shape of small polaron absorption bands agree well with the experimental data for reduced LN crystals [7, 13]. Experimental studies of electrical conductivity [18] as well as ESR studies of irradiated and reduced LN crystals [12, 15, 19, 20] also confirm the polaron nature of the absorption centres. It should be noted, that some researchers also consider the possibility of a complex nature of the induced absorption, i.e. that it is caused by both the defects in the anion sublattice and bipolarons [14, 22].

In spite of the prevailing opinion about the polaron nature of absorption of the reduced crystals, some new experimental works have appeared that testify to a participation of defects in the anion sublattice in the induced absorption. Such a conclusion was made for example on the basis of experimental observations in respect to changes in optical and electro-physical properties caused by the injection of lithium and oxygen vacancies into the crystals upon annealing in an argon atmosphere with an applied electric field [9]. The same conclusion concerning the nature of the induced absorption was also reached by studying the optical spectra of LN crystals after implantation of argon ions [21].

In most cases, the changes in optical absorption that take place in LN crystals upon high-temperature treatments have been studied at room temperature after a certain cooling procedure. That means that the changes that take place directly during the cooling process escape observation. We know of only two publications [23, 24], where *in situ* investigations of optical absorption were carried out for Fe-doped LN crystals in the spectral region of absorption of the Fe ions, however in a narrow temperature range.

The present work was undertaken to obtain more information about growth and bleaching of the induced optical absorption in LN. This paper reports on an experimental *in situ* study

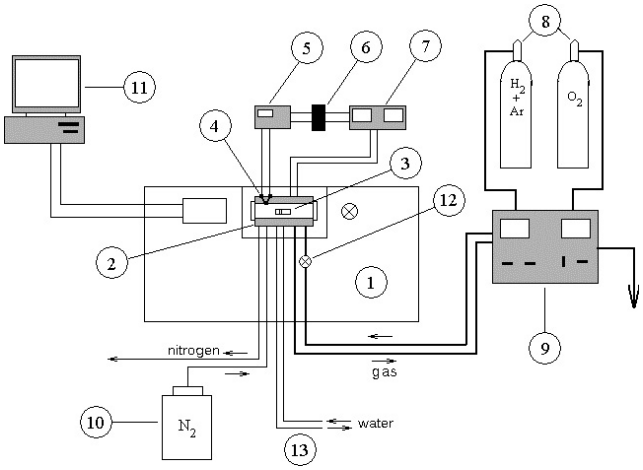

Figure 1. Scheme of the experimental set-up: 1—a spectrophotometer, 2—a resistance heater, 3—the sample on a holder, 4—the thermocouple, 5—a voltmeter, 6—a temperature controller, 7—a power supply, 8—gas cylinders, 9—the gas flow controller, 10—the liquid nitrogen cooling system, 11—a computer, 12—a gas valve, 13—the water cooling system.

of the processes at high temperatures during reducing/oxidizing treatments of LN crystals at temperatures up to 800 °C as well as during and after rapid changes in the atmospheres surrounding the samples at a fixed elevated temperature. In the latter case, a 95% Ar + 5% H_2 mixture was used as the reducing atmosphere and pure O_2 gas as the oxidizing one. Additionally, experiments using a pure argon atmosphere were carried out for comparison.

2. Experimental details

Samples for investigation were congruent $LiNbO_3$ single crystals grown by the Czochralski method. The growth technology is described in [25]. The samples were prepared as *Y*-cut and polished plates of 0.25–0.5 mm thickness.

The optical *in situ* experiments were performed using a specially designed high-temperature furnace incorporated into a Perkin-Elmer Lambda 900 spectrophotometer. A schematic diagram of the experimental set-up is shown in figure 1. The spectral range of the spectrophotometer extends from about 200 to 3000 nm (50 000–3333 cm^{-1}). The furnace allows one to heat samples from room temperature up to about 900 °C in arbitrary gas atmospheres. A temperature controller ensures a linear heating program with the maximum rate of 5 K min^{-1} as well as temperature stabilization at desired temperatures. A Pt–PtRh thermocouple was placed in the close vicinity of the sample. The gas supply system provides a predefined atmosphere in the furnace. A main feature of the set-up is the possibility of rapid (∼1 min) replacement of gas atmospheres in the furnace and of the registration of the subsequent reduction/oxidation (redox) kinetics at a given wavelength.

The heating chamber containing the sample and sample holder is about 120 mm in length and 16 mm in diameter. Both ends are hermetically closed by quartz windows. The gas flow through the furnace is about 50 cm^3 min^{-1}. The heating chamber and the holder construction ensure high homogeneity of temperature in the optically detected area of the sample that is about 2 mm in diameter.

It should be noted that the high-temperature absorption spectra were always corrected for the radiation emitted by the sample and the furnace walls. For this purpose, at each

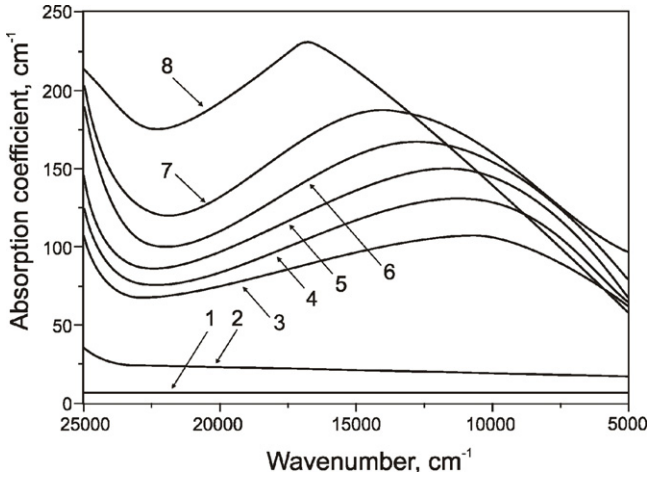

Figure 2. Optical absorption spectra of lithium niobate crystal during reducing heating: 1—at room temperature, 2—500 °C, 3—590 °C, 4—610 °C, 5—625 °C, 6—635 °C, 7—660 °C, 8—690 °C.

temperature above 400 °C an emission spectrum was registered in the absence of light from the lamp of the spectrophotometer. The experimental quantity measured is the absorbance given by $A = \log(I_0/I)$, where I_0 and I denote the intensity of incoming and transmitted light, respectively. Corrections for reflections from the sample surfaces were not made. The absorption coefficient of the crystal was calculated as $\alpha = \ln(I_0/I)/d$, where d is thickness of the crystal plate.

3. Experimental results and discussion

Figure 2 shows the absorption spectra of an LN single crystal recorded at different temperatures during stepped heating in a reducing atmosphere. Each spectrum was registered after a saturation of observed absorption changes at each temperature. The fundamental absorption edge of the crystal at room temperature is located near 35 000 cm^{-1} (at that point the absorption coefficient has a value of 150 cm^{-1} at 32 500 cm^{-1}). As the temperature increases, the fundamental absorption edge shifts towards the low-energy region. To determine this shift the absorption spectra were quickly registered in a narrow spectral range near the absorption edge with small steps of temperature increase, and the edge position was estimated for the absorption value $\alpha = 150$ cm^{-1}. This value was chosen as optimal for registration owing to the sample's thickness used. The temperature dependence of the α_{150} position is linear in the temperature range from room temperature to about 600 °C (see figure 3). The temperature coefficient $d\alpha_{150}/dT$ estimated in such a way is given by 1.43×10^{-3} eV K^{-1} (11.53 cm^{-1} K^{-1}) at temperatures up to 600 °C. Note that the thermal expansion of the crystal was not taken into account. In consequence of heating in the reducing atmosphere, the temperature dependence of the α_{150} position deviates from linearity at $T > 600$ °C because of the increasing colouration of the crystal.

As is seen from figure 4(a), the wide absorption band with its maximum near 10 000 cm^{-1} increases in intensity with increasing temperature starting from 450 °C. Figure 4(a) illustrates the growth of the absorption of the band as a function of temperature. The form of this dependence allows us to suppose that the intensity increase is of activated character. However, it is impossible to determine the parameters of the formation process of the absorption centres

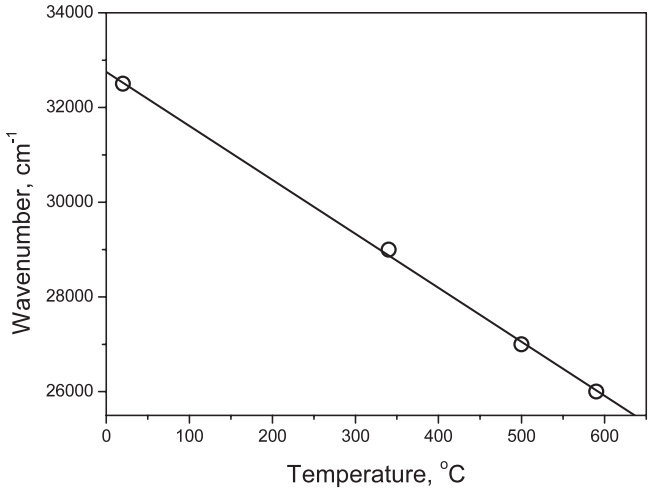

Figure 3. Temperature dependence of the fundamental absorption edge position determined for absorption coefficient $\alpha = 150\ \text{cm}^{-1}$.

because the absorption in the band with maximum at 10 000 cm^{-1} continues to grow even at constant temperature. Such a behaviour can be explained by the fact that the formation of the absorption centres involves continuously occurring diffusion processes that are sluggish in comparison to the applied heating rate.

Further heating of the crystal in reducing atmosphere leads to the appearance of one more absorption band at the high-energy side of the 10 000 cm^{-1} band. The maximum of this band, hereafter named the high-energy band, is located close to 16 000 cm^{-1} at about $T = 700\,^{\circ}\text{C}$. In particular, it is due to the formation of this band that the shift of the absorption edge with temperature is no longer linear at temperatures above 600 °C. The intensity increase of this absorption band takes place in a rather narrow temperature interval, as is shown in figure 4(b).

Replacement of the reducing atmosphere by an oxidizing one at high temperatures leads to bleaching of the absorption bands, i.e. the crystal becomes colourless again. A cycling of the atmospheres at high temperature from oxidizing to reducing (and vice versa) results in the appearance and bleaching of the respective bands. The kinetics of these processes, hereafter named reduction/oxidation kinetics, for both the absorption bands (low- and high-energy bands) at certain temperatures are shown in figures 5–8. As is seen, the rate of the reduction/oxidation processes increases with increasing temperatures for both the absorption bands.

The reduction kinetics for the low-energy band (registered at 10 000 cm^{-1}) for $T \geqslant 600\,^{\circ}\text{C}$ show some accelerating tendency instead of saturation; this is seen in particular as curve 5 in figure 5. Most likely, this is caused by a contribution of the high-energy band to the absorption registered at 10 000 cm^{-1}. On the other hand, the oxidation kinetics registered at 10 000 cm^{-1} show some slowing down after some time of the process occurring at $T \geqslant 600\,^{\circ}\text{C}$ (see figure 6) that is probably also caused by a contribution of the high-energy band to the absorption measured at 10 000 cm^{-1}.

The reduction kinetics for the high-energy band (registered by us at 14 500 cm^{-1}) reveals different values of the induced absorption that is reached at different temperatures (see figure 7). This can be explained by the fact that the wavenumber of 14 500 cm^{-1} chosen for registration of this band does not always correlate with the band maximum. As was shown above (figure 2), the band maximum shifts rapidly to the shortwave region with increasing temperatures.

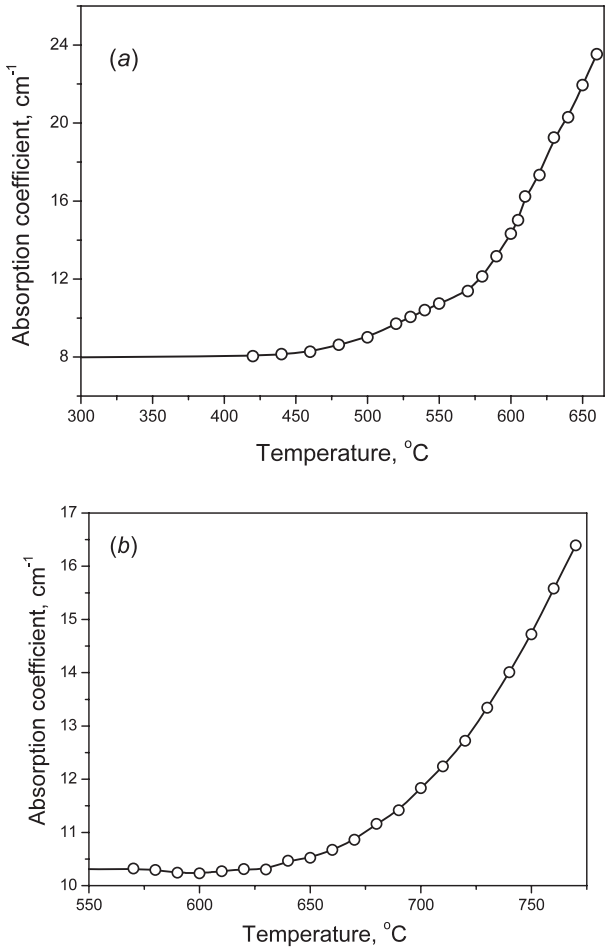

Figure 4. The optical absorption registered at 10 000 cm^{-1} (a) and at 16 000 cm^{-1} (b) as a function of temperature during heating in a reducing atmosphere.

The main peculiarity of the oxidation kinetics for the high-energy band is that the kinetics in the temperature range 600–650 °C differ essentially from the kinetics at $T > 650$ °C; see figure 8. We explain the complex shape of the kinetic curves at 600–650 °C by a superposition of the two absorption bands, which are of similar intensity in this temperature range. As the temperature increases, the high-energy band becomes dominant and the kinetics take the form that is characteristic for the high-energy band.

We have attempted to describe the observed redox kinetics by an exponential dependence like

$$A(t) = A_0 + C\exp(-t/\tau), \tag{1}$$

where C is a constant. This can be done successfully only for the high-energy band in the case of the reduction process in the reduced temperature range of 670–760 °C. We explain this by the fact that only in this case do a single absorption band and a single process dominate. The time constant τ obtained in this way exhibited an Arrhenius behaviour (figure 9) with an activation energy of about 3.4 eV.

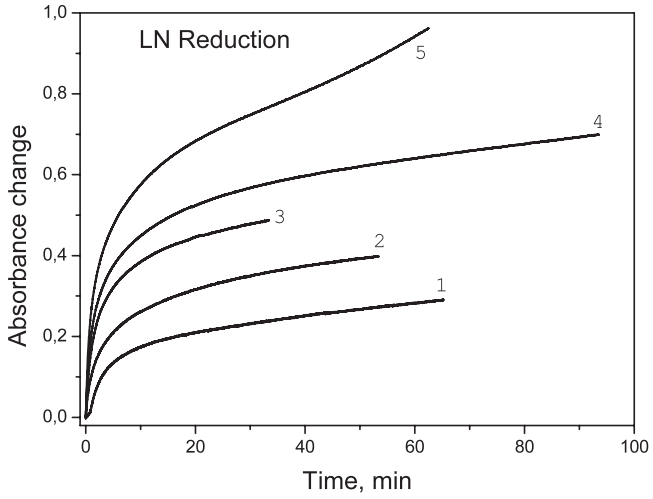

Figure 5. Time-dependent absorbance change of a lithium niobate crystal during reduction registered at 10 000 cm^{-1} at various temperatures: 1—500 °C, 2—520 °C, 3—550 °C, 4—580 °C, 5—600 °C.

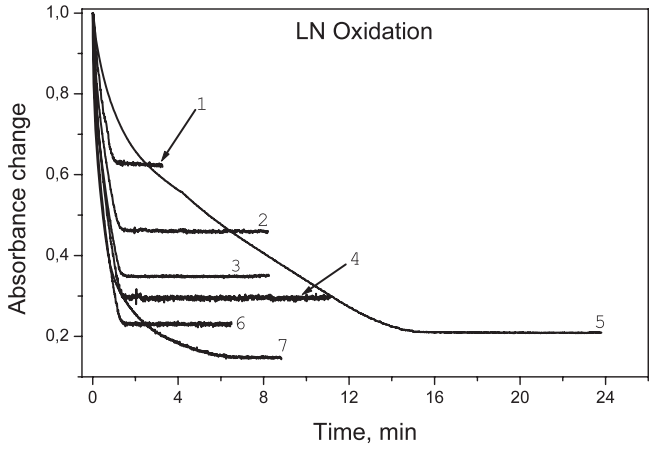

Figure 6. Time-dependent absorbance change of a lithium niobate crystal during oxidation registered at 10 000 cm^{-1} at various temperatures: 1—500 °C, 2—520 °C, 3—540 °C, 4—550 °C, 5—550 °C after four annealing cycles, 6—580 °C, 7—600 °C. Initial points are shifted for all curves to same value.

We have also tried to describe the redox kinetics in the framework of a diffusion model. In this model, we suppose that the rate of formation/disappearance of the absorption centres is determined by diffusion processes, i.e. the optical density is directly proportional to the total amount of the diffusing substance. Under the assumption that the surface concentration of the diffusing substance is constant and equal to the equilibrium concentration N_0 ($t \to \infty$) of the diffusing substance in the crystal, the time dependences of the optical density $\Delta A(t)$ may be written as [26]

$$\Delta A(t) = \beta N_0 d \frac{8}{\pi^2} \sum_{k=0}^{\infty} \frac{1}{(2k+1)^2} \exp\left(-D\frac{(2k+1)^2\pi^2}{d^2}t\right), \tag{2}$$

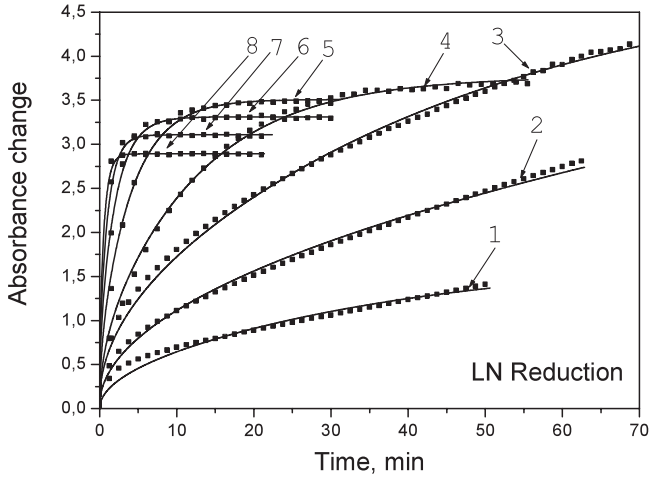

Figure 7. Time-dependent absorbance change of a lithium niobate crystal during reduction registered at 14 500 cm^{-1} at various temperatures and their theoretical approximations (solid curves): 1—600 °C, 2—630 °C, 3—650 °C, 4—670 °C, 5—690 °C, 6—710 °C, 7—740 °C, 8—760 °C.

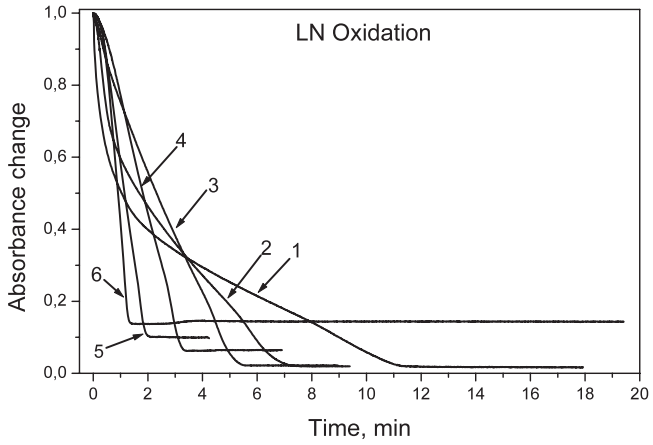

Figure 8. Time-dependent absorbance change of a lithium niobate crystal during oxidation registered at 14 500 cm^{-1} at various temperatures: 1—600 °C, 2—650 °C, 3—670 °C, 4—710 °C, 5—740 °C, 6—760 °C. The initial point is shifted for all curves to same value.

$$\Delta A(t) = \beta N_0 d \left[1 - \frac{8}{\pi^2} \sum_{k=0}^{\infty} \frac{1}{(2k+1)^2} \exp\left(-D \frac{(2k+1)^2 \pi^2}{d^2} t \right) \right] \tag{3}$$

for the cases of oxidation and reduction respectively. In (2) and (3) d is the crystal thickness, D a diffusion coefficient, and β is a coefficient connected with the absorption cross section σ by $\beta = \sigma / \ln 10$.

The kinetic curves were approximated by expressions (2) and (3) with the diffusion coefficient D and the coefficient $k = \beta N_0 d$ as fitting parameters. The fitting accuracy is

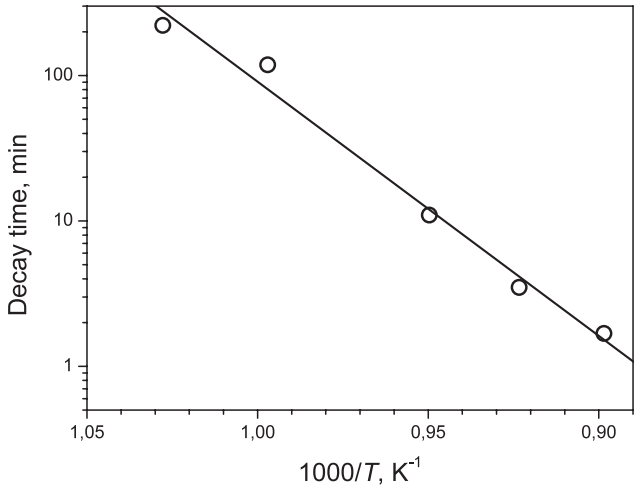

Figure 9. Arrhenius plot of the temperature-dependent relaxation times for the reduction processes registered at 14 500 cm^{-1}.

estimated by the χ^2 criterion

$$\chi^2 = \frac{1}{N - N_{\text{var}} + 1} \sum_{i=1}^{N} (\Delta A(t_i) - \Delta A_i^{\text{exp}})^2, \tag{4}$$

where N is the number of the experimental points for which fitting is carried out, N_{var} is the number of the fitting parameters, and ΔA_i^{exp} is the experimental value of the optical density change at time t_i relative to the optical density value before the annealing start. The fitting procedure employs the method of steepest descent.

Our calculations show that this diffusion model allows us to obtain an adequate fit only for the band at 16 000 cm^{-1} during reduction, but, in contrast to the exponential approximation, for all temperatures investigated. The results of this approximation are shown in figure 7 (solid curves). The seven values of the diffusion coefficient obtained from the fitting are well approximated by a straight line in the Arrhenius plot (figure 10). Only for the lowest temperature (600 °C) is the obtained diffusion coefficient not in agreement with the Arrhenius dependence. This is not astonishing because of the low quality of the approximation to the kinetic curve at this temperature (curve 1 in figure 7). Also, it can be connected with the fact that, at low temperatures (600 °C), the contribution of the low-energy band is essential. The calculated activation energy for the diffusion coefficient is given by 3.61 ± 0.36 eV and the diffusion coefficient changes from 4.03×10^{-9} cm^2 s^{-1} at 630 °C to 1.72×10^{-6} cm^2 s^{-1} at 760 °C. The value of the activation energy is close to that obtained in the case of the exponential dependence.

One more peculiarity observed experimentally should be noted. After repeated redox processes at relatively high temperature ($T \geqslant 600$ °C), the redox kinetics observed at lower temperature are essentially changed—they become slower, as shown for example by curve 5 in figure 6. Such changes in the redox kinetics can possibly be caused by irreversible changes in the structure of the near-surface region of the crystal caused by the high-temperature treatments. Therefore, all the experimental kinetics curves presented above were received for one sample step by step in one heating process—the sample was heated in reducing atmosphere to a certain temperature, where oxidation and reduction kinetics were recorded; after that the crystal was

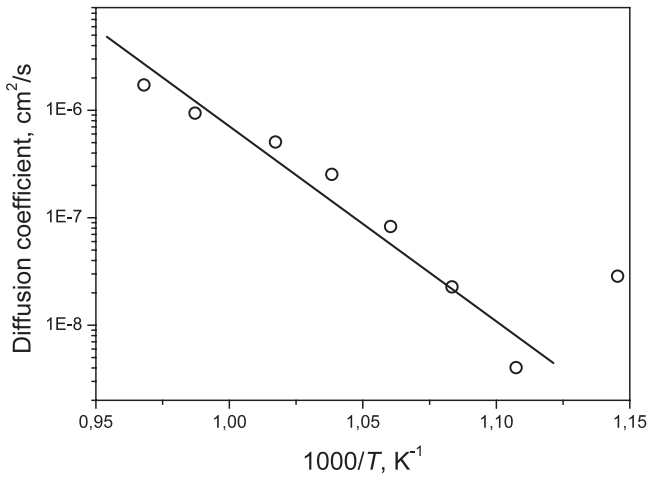

Figure 10. Arrhenius plot of the temperature dependences of the diffusion coefficient for the reduction processes registered at 14 500 cm^{-1}.

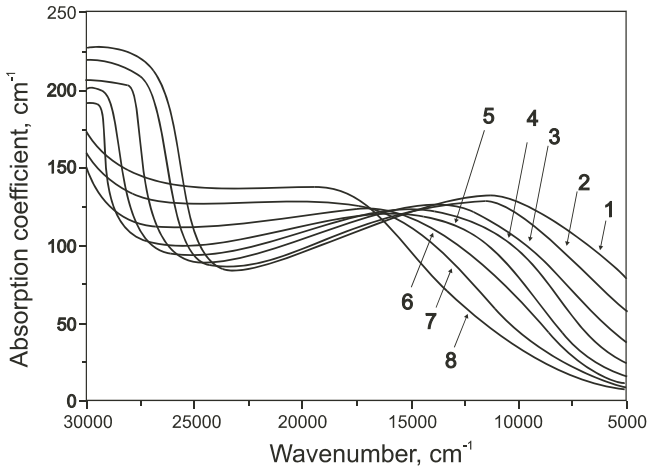

Figure 11. Optical absorption spectra of lithium niobate crystal during cooling from 590 °C to room temperature in reducing atmosphere: 1—590 °C, 2—500 °C, 3—415 °C, 4—340 °C, 5—245 °C, 6—165 °C, 7—80 °C, 8—at room temperature.

heated in reducing atmosphere to the next (upper) temperature, and so on, up to the maximum temperature used.

An interesting feature is observed when the crystal is cooled down in reducing atmosphere. If the crystal is cooled down from 600 °C, when only the low-energy band is observed, this band bleaches during the cooling and the band in the high-energy side instead arises. As a result, only one absorption band with maximum near 20 000 cm^{-1} remains at room temperature (figure 11). We believe that this is the same high-energy band, which has the maximum near 16 000 cm^{-1} at higher temperature.

However, if the crystal is cooled from 800 °C down to room temperature in reducing atmosphere, the structure of the spectrum does not change, i.e. both bands remain. Only a blue shift of band maxima is observed as temperatures decrease. We have also confirmed

experimentally that a pure argon atmosphere applied at high temperature subsequently to the treatment in 95% Ar + 5% H_2 causes the bleaching of the low-energy band. However, the duration of such an 'oxidation' process takes much longer in the pure argon atmosphere than in an oxygen atmosphere due to its much lower oxygen partial pressure, of the order of 10^{-4}–10^{-5} atm. On the other hand, the replacement of gas atmospheres from oxygen to argon and vice versa at temperatures up to 800 °C does not change the crystal absorption registered at 10 000 cm^{-1}, i.e. the crystal remains colourless in this spectral region.

Based on these observations, it is concluded that the formation of the low-energy absorption band during annealing in the 95% Ar + 5% H_2 atmosphere is connected with the incorporation of hydrogen ions into the crystal. The subsequent bleaching of this band in an oxidizing or neutral atmosphere is explained by the removal of the hydrogen ions from the crystal. The fact that the low-energy band is formed first at moderate temperature can be taken as indirect evidence of this supposition. Owing to their small radius, their higher activity and mobility, diffusion of H^+ ions can be expected to take place first. Electrons that are set free during the incorporation of H^+ ions into the crystal can form small polarons responsible for the absorption band at around 10 000 cm^{-1} [11, 15, 16].

On the other hand, the formation/bleaching of the high-energy absorption band is correlated with the removal/incorporation of oxygen from the crystal. Electrons that became free during oxygen removal can lead to formation of bipolarons or F-type centres that can be responsible for the absorption band at 20 000 cm^{-1}. Moreover, the experimental results presented above testify to a retrapping of electrons from the small polarons to the centres absorbing near 20 000 cm^{-1} (bipolarons or F-type centres) during cooling down of the crystal in reducing atmosphere.

4. Conclusions

An *in situ* optical spectroscopy study of congruent lithium niobate is reported for reducing (95% Ar+5% H_2) and oxidizing (O_2) high-temperature treatments in the temperature range 20–800 °C. It was shown that the crystal colouration occurring during reduction takes place in two stages. In the first stage a low-energy absorption band (maximum near 10 000 cm^{-1}) appears in the temperature range 450–600 °C. Further heating of the crystal in reducing atmosphere leads to the formation of a high-energy absorption band (centred at 16 000 cm^{-1} at about $T = 700$ °C).

If the crystal is cooled down in reducing atmosphere from 600 °C, when only the low-energy band is observed, this band bleaches and the high-energy band instead arises during cooling. Thus, only the high-energy absorption band that has maximum near 20 000 cm^{-1} remains at room temperature. If the crystal is cooled down from 800 °C, with both bands observed, the structure of the spectrum does not change down to room temperature, i.e. both bands remain at room temperature.

A replacement of the reducing atmosphere by an oxidizing one and vice versa at high temperature leads to bleaching/formation of the absorption bands. An attempt to describe the reduction kinetics observed for the high-energy band in the framework of diffusion processes yields diffusion coefficients ranging from 4.0×10^{-9} $cm^2\ s^{-1}$ at $T = 630$ °C to 1.7×10^{-6} $cm^2\ s^{-1}$ at $T = 760$ °C with an activation energy of 3.6 eV.

It is concluded that the increase of the low-energy absorption band during annealing in 95% Ar+5% H_2 atmosphere starting from 450 °C could be correlated with the incorporation of hydrogen ions into the crystal. On the other hand, the formation of the high-energy absorption band at temperatures above 600 °C is attributed to the removal of oxygen from the crystal.

Acknowledgments

The work was partially supported by BMBF (project UKR02/016) and by Ukrainian Ministry of Education and Science (projects 'Cation' and M/11-2004). D Sugak and Yu Sugak gratefully acknowledge the financial support provided by DAAD.

References

[1] Arizmendi L 2004 *Phys. Status Solidi* a **201** 253
[2] Buse K, Adibi A and Psaltis D 1998 *Nature* **393** 665
[3] Volk T R and Rubinina N M 1988 *Phys. Status Solidi* a **108** 437
[4] Adibi A, Buse K and Psaltis D 1999 *Appl. Phys. Lett.* **74** 3767
[5] de Miguel-Sanz E M, Carrascosa M and Arizmendi L 2002 *Phys. Rev.* B **65** 165101
[6] Buse K, Breer S, Peithmann K, Gao M and Krätzig E 1997 *Phys. Rev.* B **56** 1225
[7] Jhans H, Honig J M and Rao C N R 1986 *J. Phys. C: Solid State Phys.* **19** 3649
[8] Arizmendi L, Cabrera J M and Agulló-López F 1984 *J. Phys. C: Solid State Phys.* **17** 515
[9] Bredikhin S, Scharner S, Klinger M, Kveder V, Red'kin B and Weppner W 2000 *J. Appl. Phys.* **88** 5687
[10] Bordui P F, Jundt D H, Standifer E M, Norwood R G, Sawin R L and Galipeau J D 1999 *J. Appl. Phys.* **85** 3766
[11] Kitaeva G Kh, Kuznetsov K A, Morozova V F, Naumova I I, Penin A N, Shepelin A V, Viskovatich A V and Zhigunov D M 2004 *Appl. Phys.* B **78** 759
[12] Sweeney K L, Halliburton L E, Bryan D A, Rice R R, Gerson R and Tomaschke H E 1985 *J. Appl. Phys.* **57** 1036
[13] Dhar A and Mansingh A 1990 *J. Appl. Phys.* **68** 5804
[14] García-Cabañes A, Sanz-García J A, Cabrera J M, Agulló-López F, Zaldo C, Pareja R, Polgár K, Raksányi K and Fölvàri I 1988 *Phys. Rev.* B **37** 6085
[15] Schirmer O F 2000 EPR investigations of small electron and hole polarons in oxide perovskites *Defects and Surface-induced Effects in Advanced Perovskites* ed G Borstel (Amsterdam: Kluwer–Academic) pp 75–88
[16] Schirmer O F, Thiemann O and Wöhlecke M 1991 *J. Phys. Chem. Solids* **5** 185
[17] Wilkinson A P, Cheetham A K and Jarman R H 1993 *J. Appl. Phys.* **74** 3080
[18] Dhar A and Mansingh A 1991 *J. Phys. D: Appl. Phys.* **24** 1644
[19] Dutt D A, Feigl F J and DeLeo G G 1990 *J. Phys. Chem. Solids* **51** 407
[20] Schirmer O F and von der Linde D 1978 *Appl. Phys. Lett.* **33** 35
[21] Lu M, Makarenko B N, Hu Y-Z and Rabalais J W 2003 *J. Chem. Phys.* **118** 2873
[22] García-Cabañes A, Diéguez E, Cabrera J M and Agulló-López F 1989 *J. Phys.: Condens. Matter* **1** 6453
[23] Panatopoulos G, Luenemann M, Buse K and Psaltis D 2002 *J. Appl. Phys.* **92** 793
[24] Yükselici M H, Allahverdi Ç and Tunç A V 2004 *Phys. Status Solidi* b **241** 3041
[25] Solskii I M, Sugak D Yu and Gaba V M 2005 *Tekhnologiya i Konstruirovanie v Elektronnoy Apparature* **5** 51 (in Russian)
[26] Crank J 1958 *The Mathematics of Diffusion* (Oxford: Oxford University Press)